Supplementary Materials

# High affinity binding of phosphatidylinositol-4-phosphate by *Legionella pneumophila* DrrA

Running title: Molecular basis of PtdIns(4)P-binding by DrrA

Stefan Schoebel, Wulf Blankenfeldt, Roger S. Goody* and Aymelt Itzen[#§]

Affiliation:

Max Planck Institute of Molecular Physiology

Department of Physical Biochemistry

Otto-Hahn-Strasse 11

44227 Dortmund

Germany

* Co-corresponding author: Roger S. Goody; +49 231 1332300; Fax: +49 231 1332399;

E-mail: roger.goody@mpi-dortmund.mpg.de

[#] Corresponding author: Aymelt Itzen; phone: +49 231 1332305; Fax: +49 231 1332399;

E-mail: aymelt.itzen@mpi-dortmund.mpg.de

[§] to whom correspondence should be addressed

Supplementary Methods

## Influence of Rab1b on DrrA:PtdIns(4)P affinity

All measurements were carried out at 25°C in a buffer that contained 20 mM HEPES pH 8.0, 50 mM NaCl and 2 mM DTT. Kinetic measurements were performed with a stopped-flow apparatus (Applied Photophysics). For BODIPY-PtdIns(4)P displacement from a complex with $DrrA_{340-647}$ or Rab1b:$DrrA_{340-647}$ (200 nM) or using di-C4-PtdIns(4)P, time-dependent changes in fluorescence polarization were monitored with a 570-nm cutoff filter in the stopped-flow machine, excited at 546 nm. The influence of Rab1b-binding was investigated in the presence of 10 µM Rab1b:GDP/ 50µM GDP or 10 µM Rab1b:GDP / 50 µM GTP, respectively. These conditions were carefully chosen to ensure effective ternary complex formation between Rab1b, nucleotide and DrrA based on published constants for the affinities between these molecules (Schoebel et al, 2009).

## Melting point analysis using circular dichroism

The proteins were diluted to a final concentration of 2 µM into buffer (5 mM potassium phosphate pH 7.5) and circular dichroism was recorded at 222 nm wavelength on a J-815 Spectropolarimeter (Jasco UK). The stability of the native and the mutant proteins were compared by recording denaturation curves between 20°C and 95°C. The data were converted into mean residue ellipticity (Myers et al, 1997) and analyzed using Origin 7.0.

Supplementary Figures

Supplementary Figure 1

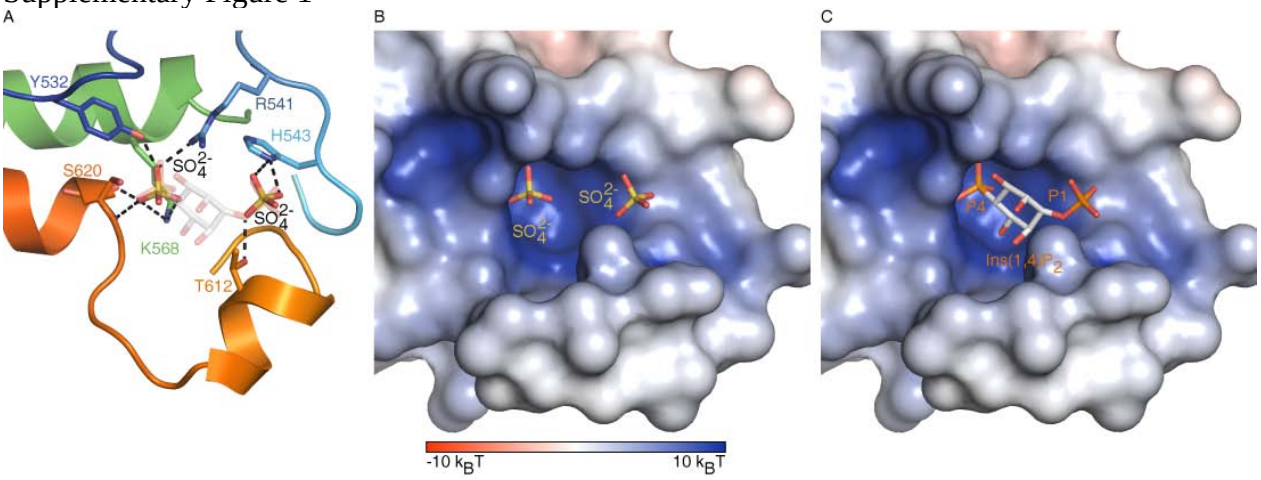


Supplementary Figure 1: The spacing of sulfate ions in the DrrA P4M crystal structure corresponds to the distance of the phosphates of PtdIns(4)P. (A) The presumable PtdIns(4)P binding pocket of the P4M is shown in cartoon representation with interacting amino acids and the sulfate ions drawn as sticks. (dashes: polar interactions). One possible conformation of the PtdIns(4)P head group is shown as semitransparent sticks to demonstrate that the spacing of the two sulfate ions corresponds very well with the distance of the phosphates in inositol 1,4 diphosphate (PtdIns(4)P head group). (For clarity, only secondary structure elements involved in binding pocket formation are shown). (B) and (C) Surface representation of the binding pocket shown in (A) colored by the electrostatic surface potential (surface potential from -10 $k_BT$ to 10 $k_BT$). The positions of the sulfate ions (B) and the presumable position of the PtdIns(4)P head group (inositol 1,4 diphosphate: Ins(1,4)$P_2$) are shown as sticks.

Supplementary Figure 2

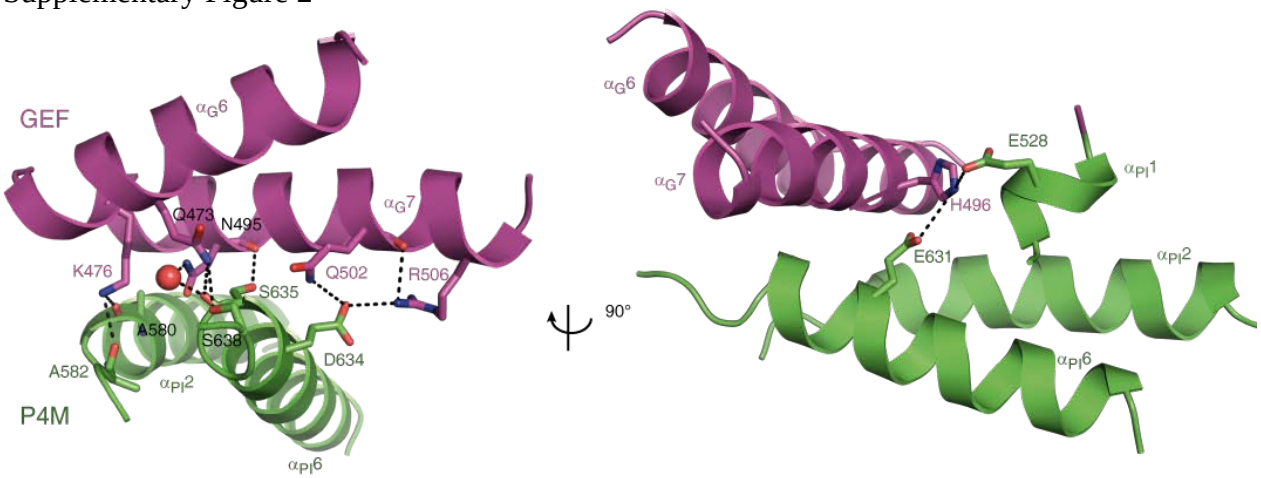


Supplementary Figure 2: Intramolecular interactions between the P4M- and GEF-domains of DrrA. Cartoon representation of the DrrA GEF-P4M crystal structure in two different views rotated by 90° (GEF: purple, P4M: green). The interacting region is shown and demonstrates the polar interactions between the GEF- and P4M-domains. (dotted lines: polar interactions, sticks: selected interacting amino acids, red sphere: water molecule involved in polar interactions of the interface). Secondary structure elements not involved in the interface formation are not shown for clarity.

Supplementary Fig 3

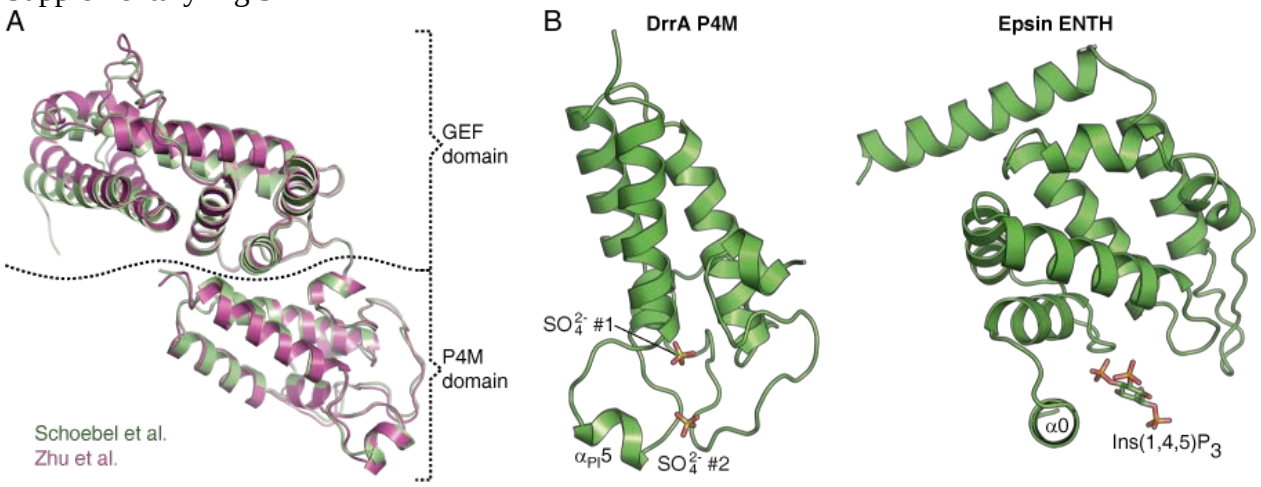


Supplementary Figure 3: Structural comparisons of different phospholipid binding proteins. (A) A structural superimposition of our structure (purple) and the $DrrA_{317-647}$ structure (Zhu et al, 2010) is shown. The superimposition was performed with the P4M domains only. The root-mean-square deviation (RMSD) of the $C_\alpha$-trace of the P4M domains is 0.64 Å, while the RMSD of the total molecule is 1.0 Å. Thus, despite crystallization under different conditions and in different space groups, the structures are highly similar. Therefore, the relative orientation of the two domains towards each other is likely to be also stable in solution or on the membrane. (B) Structural comparison of the DrrA P4M and the ENTH domain of Epsin. The figures shows the cartoon representations of the ENTH domain of Epsin (Ford et al, 2002) (right panel) and the DrrA P4M (left panel). This demonstrates that the two domains have no structural similarity aside from the all α-helical fold. However, the amphiphatic helix α0 of the ENTH domain which is implicated in membrane binding has a similar position in relation to the inositolphosphatidyl phosphate head group as the amphiphatic $\alpha_{PI}5$-helix in the DrrA P4M to the sulfates found in the presumable lipid binding pocket. This strengthens the notion that the $\alpha_{PI}5$-helix could be involved in membrane binding of the DrrA P4M. (The inositolphosphatidyl phosphate head group of the ENTH domain is depicted by the Ins(1,4,5)$P_3$ found in the crystal structure (Ford et al, 2002). The orientation of the ENTH domain is shown similarly to (Lemmon, 2008).)

Supplementary Fig 4

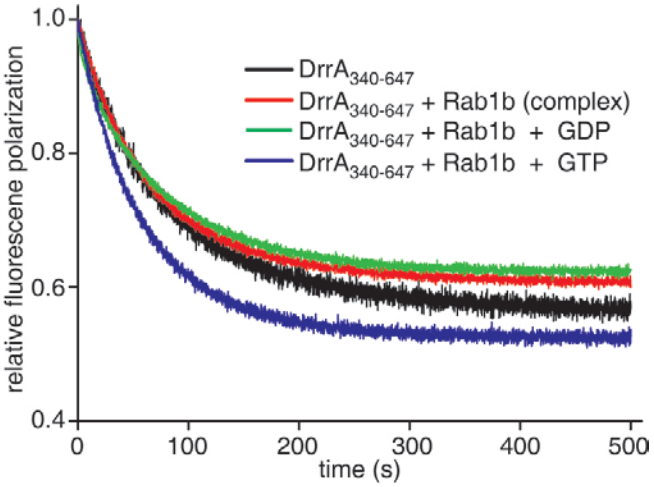


Supplementary Figure 4: Rab1b has no significant influence on the dissociation rate of the complex between $DrrA_{340-647}$ and BODIPY-PtdIns(4)P. The time-resolved dissociation of BODIPY-PtdIns(4)P from $DrrA_{340-647}$ in the presence of Rab1b, Rab1b:GDP or Rab1:GTP was monitored to analyze the influence of Rab1-DrrA interaction on the DrrA:PtdIns(4)P-complex affinity using stopped-flow. BODIPY-PtdIns(4)P (200 nM) was displaced from $DrrA_{340-647}$ (200 nM) by shooting against unlabeled PtdIns(4)P (2 µM) (black curve). The experiment was repeated in the presence of 10 µM Rab1:GDP/50 µM GDP (green curve) or 10 µM Rab1:GDP/50 µM GTP (blue curve) or with the 200 nM nucleotide-free Rab1b:$DrrA_{340-647}$-complex (red curve). The rate of displacement of BODIPY-PtdIns(4)P from $DrrA_{340-647}$ is unchanged in all experiments. Hence, Rab1b, Rab1b:GDP, and Rab1b:GTP do not significantly influence the binding between DrrA and PtdIns(4)P.

Supplementary Figure 5

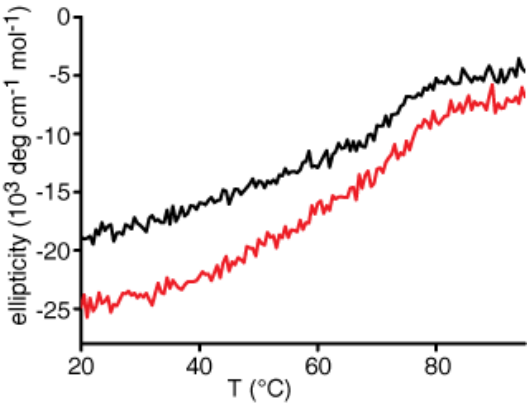


Supplementary Figure 5: Melting point analysis of $DrrA_{340-647}$ and $DrrA_{340-647}$ K568A. The thermal denaturation of 2 µM $DrrA_{340-647}$ (black curve) or $DrrA_{340-647}$ K568A (red curve) was monitored by changes in circular dichroism. No significant changes between the melting point of $DrrA_{340-647}$ and $DrrA_{340-647}$ K568A are observable, indicating that the mutation K568A does not impair protein stability.

Supplementary references

Ford MGJ, Mills IG, Peter BJ, Vallis Y, Praefcke GJK, Evans PR, McMahon HT (2002) Curvature of clathrin-coated pits driven by epsin. *Nature* **419**(6905)**:** 361-366

Lemmon MA (2008) Membrane recognition by phospholipid-binding domains. *Nat Rev Mol Cell Biol* **9**(2)**:** 99-111

Myers JK, Pace CN, Scholtz JM (1997) Helix propensities are identical in proteins and peptides. *Biochemistry* **36**(36)**:** 10923-10929

Schoebel S, Oesterlin LK, Blankenfeldt W, Goody RS, Itzen A (2009) RabGDI displacement by DrrA from *Legionella* is a consequence of its guanine nucleotide exchange activity. *Mol Cell* **36**(6)**:** 1060-1072

Zhu Y, Hu L, Zhou Y, Yao Q, Liu L, Shao F (2010) Structural mechanism of host Rab1 activation by the bifunctional *Legionella* type IV effector SidM/DrrA. *Proc Natl Acad Sci U S A* **107**(10)**:** 4699-4704